STM JOURNALS

Journal of
Polymer & Composites

ISSN: 2321-2810 (Online)
ISSN: 2321-8525 (Print)
Volume 12, Special Issue 4, 2024
DOI (Journal): 10.37591/JoPC

http://engineeringjournals.stmjournals.in/index.php/JoPC/index

Research JoPC

Stress Based Topology Optimization of Axial Tubes Under Impact to Improve Energy Absorption

Prashant Manvi[1], Fareen Nizami[2], Anandtheertha M R[3], Srikanth H V*[4]

Abstract

The present study is aimed at designing a stress constrained topology optimized tube to improve the specific energy absorption (SEA) and reduce the peak crushing force. The research was aimed to develop an axial tube to withstand high impact loads thus improving the crash worthiness of the structure. Crash analysis of a 3D deformable circular tube having different thickness of 0.5 mm, 1 mm, 1.5 mm and 2 mm with a constant inner diameter and length sandwiched between two square rigid planar shell plates was performed. SEA and Peak crushing force (PCF) were computed post the crash analysis. Stress based topology optimization was then carried out on a prismatic tube by varying the Factor of Safety from 1.2 to 2 in steps of 0.2 using the SIMP algorithm on a tube with the highest SEA. Crash analysis was carried out post the optimization process in a similar manner by varying the thickness. SEA and PCF were computed, and results show that the optimized tube with the thickness of 1 mm absorbs 933.53 J of energy with a SEA of 27.22 J/g when compared to the prismatic tube (945.74 J) of the same thickness with a SEA of 17.06 J/g.

Keywords: SEA- Specific Energy Absorption, EA- Energy Absorption, PCF- Peak Crushing Force, MCF- Mean Crushing Force, SIMP method- Solid Isotropic Material with Penalization method, FOS-Factor of Safety, UAV, GPS, Autodesk flow, Inertial Measurement Unit (IMU)

INTRODUCTION

Energy-absorbing structures are employed where collision resulting from impact may cause serious consequences such as injury or fatality to human life and damage to vehicles. When structures are subjected to collision, the external kinetic energy is dispersed largely due to plastic deformation [1]. Thin-walled tubes or structures are broadly utilized as energy-absorbers in military, aerospace and automotive industries to reduce fatality and damage to human life and to protect vital equipment from damage due to collision. Extensive research has been done to improve energy absorption capacity of thin walled tubes such as using nature inspired structure which sometimes increases mass and complexity of manufacturing the tubes, for example internal hierarchy of tendon was imitated by adding seven small tubes inside a large diameter tube and, similar hierarchy was adopted to develop honeycomb structures. Cross section and nodes of bamboo was mimicked for enhancing the crashworthiness performance of structures and a good improvement in the energy absorption was observed [2-6]. Investigation by changing the cross section of tubes such as circular, rectangle, square, hexagonal, octagonal etc. have also been carried out under axial impact loading. Straight and tapered thin walled tubes having different cross sections subjected to axial and oblique impact loading were also investigated and the comparison of energy absorption for various cross-sectional tubes

***Author for Correspondence**
Srikanth H V

[1,2]Assistant Professor, Department of Aeronautical Engineering, Nitte Meenakshi Institute of Technology, Bangalore, India.
3UG Student, Department of Aerospace Engineering, RV College of engineering, Bangalore, India.
[4]Professor, Department of Aeronautical Engineering, Nitte Meenakshi Institute of Technology,
Bangalore, India

Received Date: January 09, 2024
Accepted Date: January 19 2024
Published Date: May 13, 2024

Citation Prashant Manvi, Fareen Nizami, Anandtheertha M R, Srikanth H V. Stress Based Topology Optimization of Axial Tubes Under Impact to Improve Energy Absorption . Journal of Polymer & Composites. 2024; 12(Special Issue 4): S210–S220.

were made. In both the cases of axial and oblique impact loading, hexagonal cross section tube showed highest specific energy absorption (SEA) and square tube showed the lowest SEA. It was also noticed that the crush strength increases as the number of corners increased and it saturates when the number of corners becomes eleven [7-9]. The effect of tube length, diameter and thickness plays a significant role on the energy absorption, with the increase in length, diameter and L/D ratio the energy absorption increases whereas the effect of increase in weight is almost insignificant on the energy absorption property [10-11]. Improvement in the specific energy absorption (SEA) is observed when optimization was carried out by introducing cells in the tubes having different cross sections and by using straight or curved stiffeners and walls under both quasi-static and impact loading [12]. Improvement of 48.3% was observed in the energy absorption for a square multi-cell tube [13]. Optimization was performed to improve the SEA by including multiple cells with different orientation, introducing sandwiched pattern in square tubes, hierarchy in hexagonal tubes, designing sandwich sinusoidal lateral corrugated tubes, designing tubes using kirigami approach and press fitting steel ring on to the circular aluminium tube [14-19]. In cases of various cross sections such as square, hexagonal, rectangular, circular etc. subjected to impact loading, hexagonal cross-section having multiple cells showed highest specific energy absorption [20].

Materials also play a significant role in Specific Energy Absorption. Aluminium (AA6060-T5 and AA6060 T4) tubes performed better than magnesium alloy tubes under quasi- static loading but Magnesium tubes outperformed aluminium tubes at high speed impact and can be used for higher SEA under high strain rate conditions. It was also observed that magnesium tubes absorbed energy by fracture whereas aluminium tubes absorbed energy by yielding. The SEA of steel tubes (A 36) were found to be 4.5 times greater than aluminium tubes for all the different types of cross-sections under dynamic impact loading. The effect of strain rate on aluminium was also investigated and it was found that aluminium was strain rate insensitive [21-25].

Although extensive research has been carried out to improve energy absorption of tubes by using many novel configurations, such as multi-cell structures and foam filled structures, change in the sectional geometry of tubes and research work in topology optimization so far are formulated and solved to minimize the compliance of a structure. There is very little literature pertaining to the optimization problem considering stress as a design constraint which is realistic and acceptable from an engineering point of view. No work has been carried out using a topology optimization tool with stress constraint to improve energy absorption of the tube. Hence, the present study aims at designing a topology optimized tube having high specific energy absorption (SEA) to withstand high impact and compression loads, thus improving crashworthiness of the structure.

METHODOLOGY

The methodology adopted consists of creating a 3D model of the circular tube in ABAQUS and the crash analysis is performed with the considered dimensions having various thickness. The EA and SEA is measured from the Force vs. Displacement graphs. The folding pattern of the tubes with different thicknesses have a direct impact on the energy absorption, the effect of folding patterns of SEA is also studied. The best tube with highest SEA and lowest transmitted PF is considered and stress-based topology optimization using SIMP algorithm with varying FOS is performed. The optimized tube is developed based on the results from topology optimization. Crash analysis is then performed on the optimized tube by varying the thickness in a similar fashion to that of the prismatic tube and the tube having high SEA and lowest PCF transmitted is considered. Results from previously performed crash analysis of the prismatic circular tube and the topology optimized tube is compared.

Finite Element Modelling

A 3D deformable tube of diameter 40 mm and length 180 mm was sandwiched between two square rigid planar shell plates. The material selected was aluminium alloy AA6060-T5. The material modelling of AA6060-T5 was done as per Johnson–Cook constitutive isotropic hardening model as shown in Table 1. It is a phenomenological model that takes into account the strain hardening, strain rate effects and thermal softening. It is suitable for problems where the strain rate varies over a large range. Mass assigned to the upper plate was 0.1045 ton at a velocity of 4300 mm/s. Step is created with a time period of 0.05 to ensure there is a sufficient time to accurately predict the crushing. Interaction between the rigid impactor and the specimen is modelled using a 'node to surface' algorithm with a friction coefficient of 0.25 with a position tolerance of 3.

Table 1. Material properties of AA6060-T5

Material	Density (g/cm3)	Young's modulus (MPa)	Poisons ratio	A	B	n
AA6060-T5	2.70	69500	0.33	99.02	207.524	0.092

The upper plate which is an impactor was allowed to displace only in one translational direction i.e. in the Z direction in order to ensure that the impactor has only one translational displacement, whereas the movement of lower plate was fixed in all the direction. Based on convergence study it was found that the element size of $3\times3\text{mm}^2$ could provide accurate results and acceptable computational efficiency which is shown in graph of Figure 1. 4 node linear quadrilateral shell continuum (S4R) elements with reduced integration and hourglass control with an element size of $3\times3\text{mm}^2$ were chosen to perform the crash analysis.

Table 2. Specifications of prismatic tubes

Tube No.	Diameter (mm)	t/d ratio	Thickness (mm)	Mass(g)
1	40	0.0125	0.5	27.66
2	40	0.025	1	55.42
3	40	0.0375	1.5	83.09
4	40	0.05	2	110.67

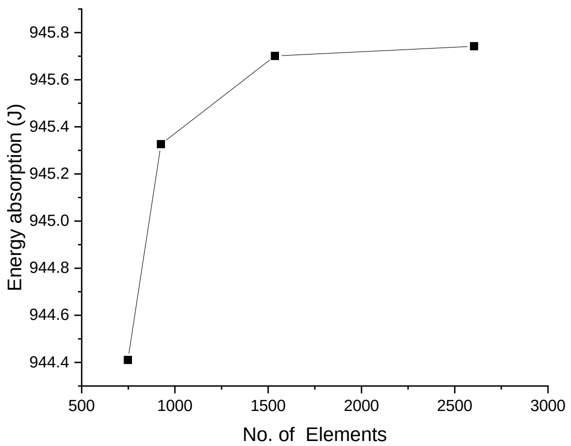

Figure 1. Variation in Energy absorption due to change in element size.

The specification of the tubes used for this study is shown in the Table 2, where the thickness of the tube is varied from 0.5 to 2mm in steps of 0.5. The maximum thickness considered is 2mm as the transition of tubes from thin shell to thick shells takes place as the t/d ratio becomes greater than 0.05.

Validation

To ensure that the developed FE model is sufficiently accurate, it is validated with previously published results. Results were validated with different thin walled tubular cross-sectional profiles such as circular, square, hexagonal, and octagonal profiles. A36 steel was used as the material to model the tube. While designing these structures, the perimeter of the cross section, the length and the thickness of the tubes were constant across all tubular profiles. The length, thickness and perimeter were 350mm, 2mm and 300mm respectively. Impact velocity and an impacting mass were 15.6 m/s and 275 kg respectively as considered by Terlochen et al. [7]. Table 3 gives the comparison between obtained results and the published results.

Table 3. Validation of results obtained with results from Terlochen et al. [7]

S N.	Profiles	Energy Absorbed reported by Tarlochen et al [7] (KJ)	Obtained Energy Absorbed (KJ)	% Deviation
1	Circular	23.67	24.64	4.09
2	Hexagon	26.67	26.19	1.79
3	Octagon	23.9	25.19	5.14
4	Square	23.22	22.79	1.85

Validation of results from Zarei et al. [26] was performed on empty tubes for five cases having different impact velocities and diameter. The tabular structure material used was aluminium alloy AA6060-T5. The comparison of results with the percentage deviation is shown in Table 4.

Table 4. Validation of results obtained.

S. N.	**Dia (mm)**	**Velocity (m/s^2)**	**Energy Absorbed reported by Zarei et al. [26] (J)**		**Obtained Energy Absorbed(J)**	**% Deviation**
			Numerical	*Experimental*	*Numerical*	
1	40	4.3	952	998	945.74	5.23
2	40	5.9	1809	1858	1817.26	2.19
3	40	6.6	2266	2326	2275.2	2.18
4	40	6.6	2270	2260	2185.92	3.27
5	40	10.7	4987	5081	4959.08	2.40

Drop weight impact analysis was carried out with mass of the impactor being 261.1 kg, drop height of 977 mm and an impact velocity of 4.4 m/s. The dimensions of the specimen were; diameter of 20 mm, Length of 20 mm, thickness of 0.5 mm, and height of 100 mm [6]. The computed results and results from Dayong et al. [6] are shown in Table 5.

Table 5. Validation of results obtained with results from Dayong et al. [6]

Particulars	**Energy Absorbed reported by Dayong et al. [6] (J)**		**Obtained Energy Absorbed (J)**	**% Deviation**
	Numerical	*Experimental*	*Numerical*	
Energy (J)	2640.8	2746	2531	4.15
SEA (J/g)	28.8	29.3	27.66	3.95

The validation of the above three reference articles was done using ABAQUS Explicit and the error found was less than 5% in all the three cases. The above papers have considered drop weight experimental testing and the same methodology was considered to carry out the numerical simulation. Quasi-static loads are not considered in this study.

Stress Based Topology Optimization

Most used objective functions in topology optimization are mass and compliance, in this study minimizing mass is the primary objective. Design variable, response and constraint are thickness, mass and stress respectively. In order to optimize a tube for maximizing energy absorption, a tube of very

Journal of Polymer & Composites
Volume 12, Special Issue 4
ISSN: 2321-2810 (Online), ISSN: 2321-8525 (Print)

high thickness is considered with an outer diameter of 40 mm and a thickness of 10mm. The contacts between tube and rigid plates is a “bonded” type contact. One plate is fixed and the other plate is subjected to a static load of 30000N, from previous findings it can be observed that peak load of around 30000 N is experienced by the tube during crash/crushing, hence the static load applied is equivalent to that of peak load experienced by the tube. The tube is assigned as design space and the plates are assigned as non-design space so that all the optimization process takes place at the tube and no modification is allowed to the plates. Objective to be achieved was minimum mass, and stress constraints given was in terms of factor of safety. Various factor of safety was considered, and optimization was performed using the SIMP algorithm. The minimum thickness considered was 5mm which is kept constant through all other optimization processes having varying factor of safety.

Topology Optimized Tubes with Different FOS

It is evident from Figure 2, that, as the FOS increases, mass increases and the compliance decreases. As the factor of safety increased the tube had to account for large amount of unexpected loading. The results obtained after topology optimization could not be directly imported for crash analysis. Hence, in order to perform the analysis, the tube with FOS 1.2 was modelled as a shell for analysis.

Figure 2. Tubes optimized for FOS 1.2, 1.6 and 1.8.

Various views of topology optimized tube with 1.2 FOS

Figure 3 and Figure 4 depicts the topology optimized tube and the corresponding basic drawings. Drawings were generated by measuring the various dimensions of the optimized tube. The length remained 180mm, but some dimensions were approximated, as the surface of the tube was highly irregular and made it difficult to measure the exact dimensions of optimized tube.

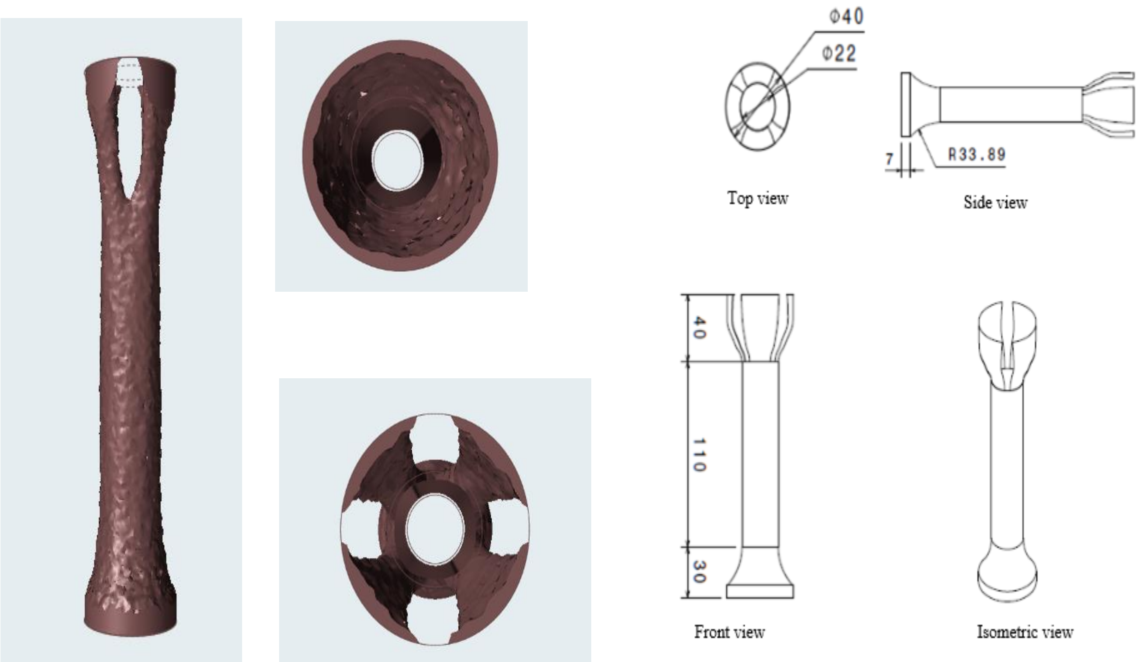

Figure 3. Topology Optimized Tube and basic drawings.

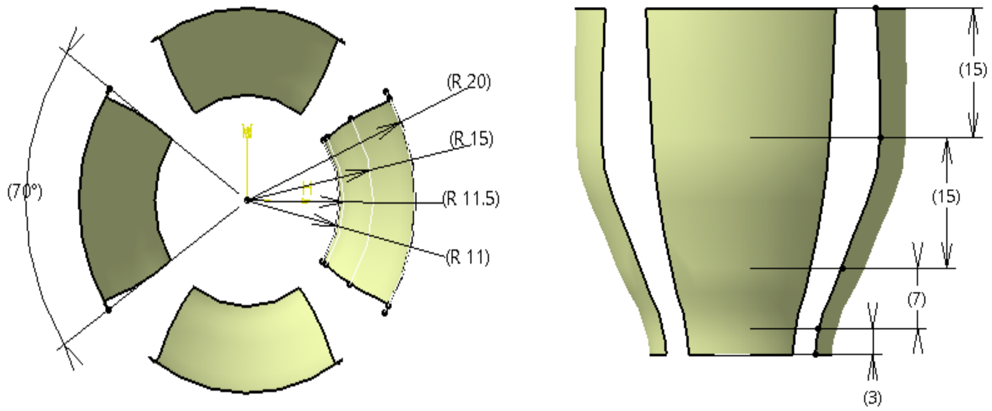

Figure 4. Flange dimensions.

RESULTS AND DISCUSSION

Prismatic Tube Results

Based on validated results of Zarei et al. [26] crash analysis was performed on the prismatic unoptimized tubes. The results obtained are tabulated in Table 6. Parameters of importance were Energy Absorbed (EA), Peak Crushing Force (PCF), Mean Crushing Force (MCF), Displacement and Specific Energy Absorption (SEA).

Table 6. Results of prismatic tube with different thicknesses

Tube no	Thickness (mm)	EA (J)	PCF (N)	MCF (N)	Displacement (mm)	SEA (J/g)
1	0.5	948.98	27566.7	8249.01	153.75	34.30
2	1	945.74	29462.9	13094.7	69.29	17.06
3	1.5	934.78	45873.3	25020.32	35.08	11.25
4	2	925.27	63124.3	37180.13	21.92	8.36

Folding pattern of the Prismatic tubes

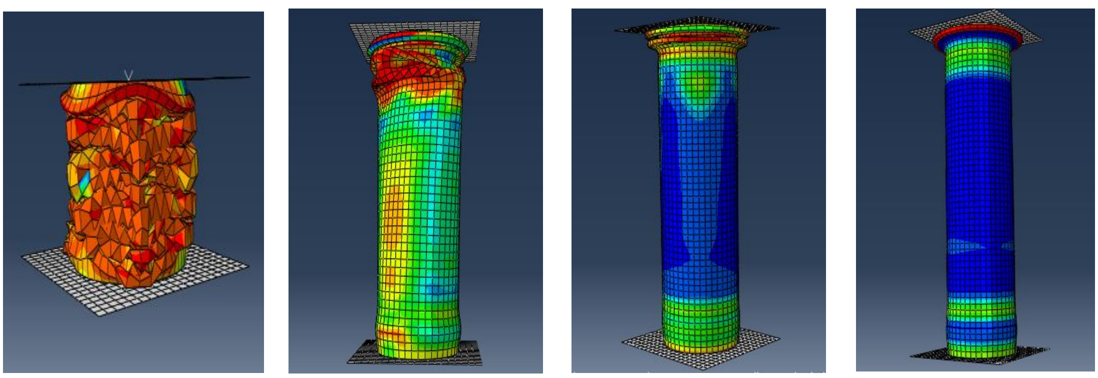

Figure 5. Folding Patterns for varying thickness from 0.5mm to 2mm.

The pattern of folding observed in 0.5 mm thickness tube was completely diamond as shown in Figure 5. Mixed pattern of folding consisting of circular folds in the beginning followed by diamond folds was observed for a tube of 1mm thickness. The tube with 1.5 mm and 2 mm thickness showed only circular folding pattern. The displacement and energy absorbed decreased with the increase in thickness of the tube. The decrease in energy absorption can also be attributed to the circular folding pattern.

Changes in the SEA, Peak force, Mean force with respect to thickness

SEA decreased with the increase in thickness which can be observed in Figure 6. PCF and MCF gradually increased from with increase in thickness depicted in Figure 7. The energy absorbing characteristic decreases as the thickness increases causing an increase in PCF and MCF.

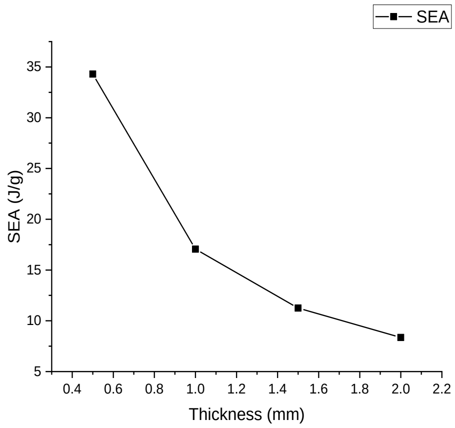

Figure 6. SEA vs. Thickness graph

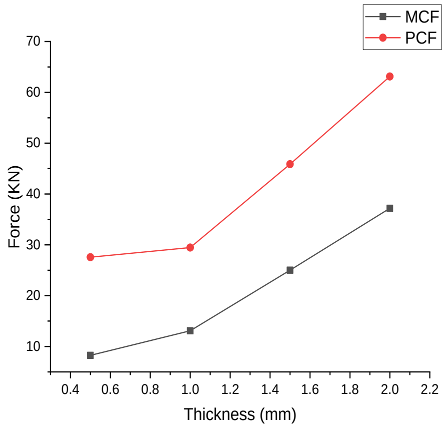

Figure 7. Force vs. Thickness graph

It can be seen from table 6 that the energy absorbed by the 0.5mm thick tube and 1mm thick tube is almost same, it can be also noted that the peak load transmitted is also similar. But it can be observed that the tube with 1mm thickness absorbed similar amount of energy with less deformation. Hence the 1mm thick tube is chosen for performing stress-based topology optimization

Force VS Displacement Graphs of Prismatic Tubes

As seen from Figure 8, the graphs follow similar pattern to that of a typical force vs. displacement graph with the PCF transmitted being maximum in the 2mm thickness tube. The 0.5 mm and 1 mm thickness tubes absorbed maximum energy of 948.98 N and 945.74 N respectively and the PCF transmitted was lower in these tubes.

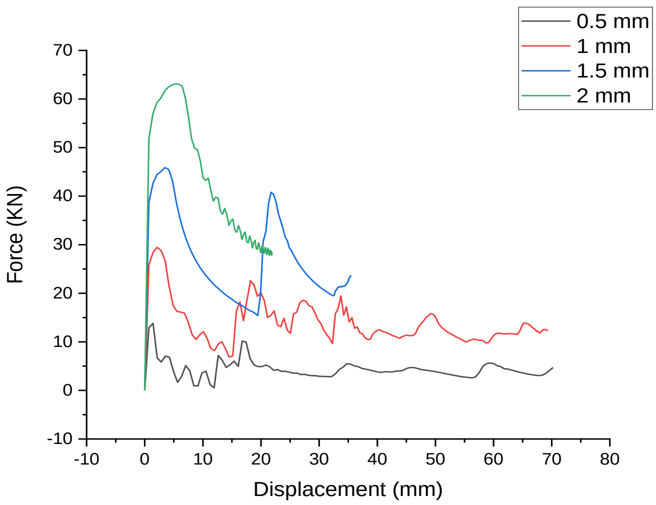

Figure 8. Force vs. displacement graphs

Optimized Tube Results

Crash analysis was carried out for the optimized tube. The boundary and loading conditions were similar to that of the crash analysis. This analysis was also performed with different thicknesses i.e. 0.5mm, 1mm, 1.5mm and 2mm. The various specifications of the optimized tube and the results obtained after crash analysis is tabulated in the Table 7.

Table 7. Results of optimized tubes with different thicknesses

Sl No	Thickness (mm)	Mass (g)	Energy absorbed (J)	PCF (kN)	MCF (kN)	Displacement (mm)	SEA (J/g)
1	0.5	17.14	964.32	10.21	9.46	173.90	56.26
2	1	34.29	933.53	16.06	7.44	142.49	27.22
3	1.5	51.34	956.16	26.30	12.86	89.24	18.62
4	2	68.49	953.11	36.70	16.47	66.93	13.91

Folding Pattern of Optimized Tubes

Diamond folds were observed for tubes with thickness 0.5mm, 1mm and 1.5mm shown in Figure 9, tube with 2mm thickness showed a buckling phenomenon. This is due to the fact that thickness of the tube is higher, and acts as resistance to crush rather than an energy absorber.

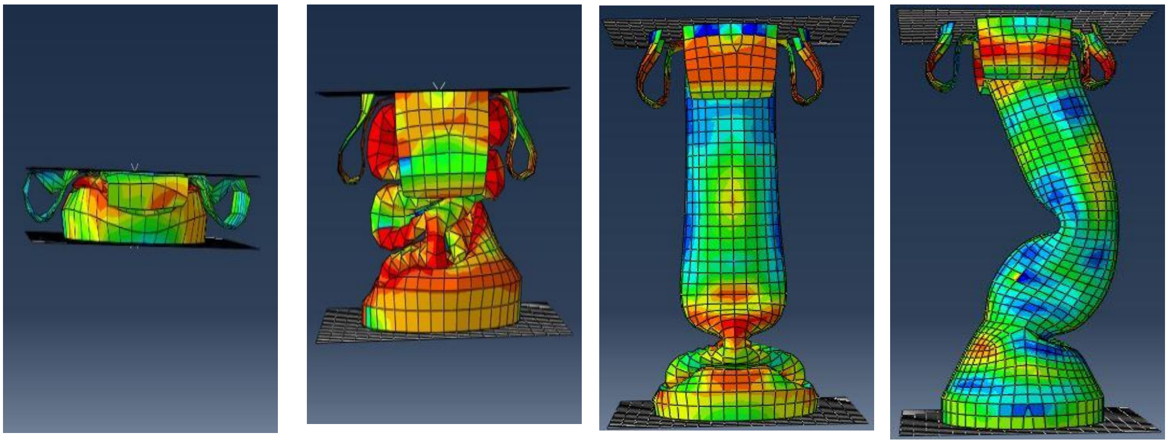

Figure 9. Folding patterns for tubes with varying thickness from 0.5mm to 2mm.

Changes in the SEA, Peak force, Mean Force of Optimized Tube with Respect to Thickness

SEA decreased with the increase in thickness which can be observed from the above graph in Figure 10. The decrement in the SEA is sharp as the thickness changes from 0.5mm to 1mm. As observed in Figure 11, PCF decreases from 0.5mm to 1mm thickness then increases gradually as the thickness is varied from 1mm to 2mm, thus at 1mm thickness peak load is minimum and at 0.5 mm it is maximum.

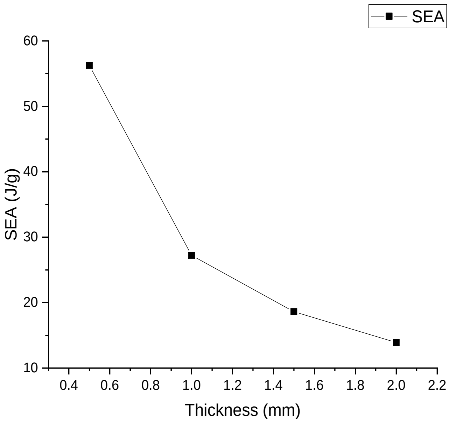

Figure 10. SEA vs. Thickness graph

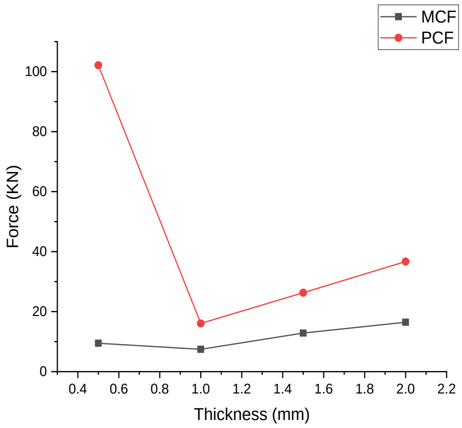

Figure 11. Force vs. Thickness graph

With respect to PCF, the tube with 1mm thickness was found to be acceptable. From the g Figure 11. It is observed that as thickness changes from 0.5 to 1mm the MCF slightly decreases then begins to increase as the thickness is varied from 1mm to 2mm.

Force VS Displacement Graphs of Optimized Tubes

The optimized tube with 0.5mm thickness performs least among all the other tube though the energy absorbed is maximum as the PCF transmitted is relatively very large. The main objective of any energy absorbing structure is to absorb maximum amount of energy and transmit the minimum amount of force. This tube fails at minimizing the amount of force transmitted to the rest of the structure, which in turn leads to the damage of other structures. The tube with 1mm thickness performed better among the four tubes as it showed lowest transmitted PCF, with a SEA similar to the 0.5mm thick tube (Figure 12).

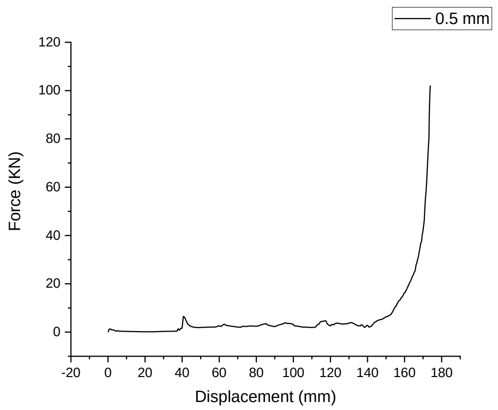

Figure 12. Force vs. Displacement graph

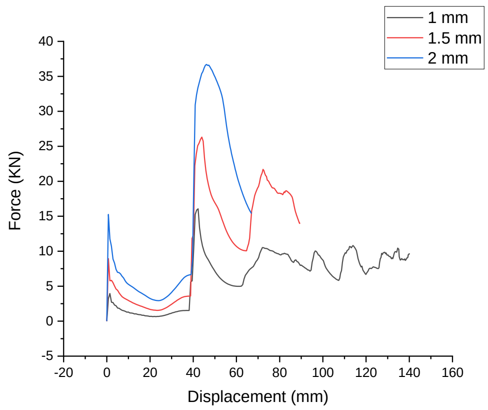

Figure 13. Force vs. Displacement graph

As observed in Figure 13 there is small peak at the beginning of the graph which corresponds to the flanges, as the flanges have low stiffness, they absorb a small amount of force before transmitting the rest to the smaller cross section tube. Absence of the flanges will make the optimized tube a prismatic tube of uniform cross section tube which will reduce the specific energy absorption to a great extent. Because with the same length, greater mass, larger outer diameter and similar boundary conditions the energy absorption was lesser in prismatic tube as per Table no. 6 whereas the optimized tube with similar length and boundary condition and in fact with the smaller diameter in majority of its portion and lesser mass in it, the energy absorption was higher as per Table no. 7. The absence of flanges at the top and bulged portion at the bottom of the optimized tube will make it a prismatic tube of diameter of 22 mm and length of 180 mm. Therefore the prismatic tube with a diameter of 20mm will absorb lesser energy than 40mm diameter. Hence, the flanges play an important role in improving the energy absorption. The PCF is highest when the displacement is 40mm which is after the flanges have deformed and the tube is under compact. It can be noticed in Figure 13. that the increase in the thickness decreases SEA, though the decrease in the EA is quite small but the decrease in SEA is noticeable.

CONCLUSION

The optimized tube performed better when compared to a prismatic tube. Optimization helped in improvement of specific energy absorption characteristics and also helped in reducing the peak load transmitted. The following conclusions can be drawn from the present study.

- The optimized tube with the thickness of 0.5mm is shown to absorb the maximum amount of energy of 964.32 J and highest SEA of 56.26 (J/g) but at the same time the PCF transmitted is very high i.e. 102135 N. Hence, it is not desirable and performs least among all the other tubes.
- The optimized tube with the thickness of 1mm is shown to absorb 933.53 J of energy which is

comparatively smaller than others but the SEA is higher i.e. 27.22(J/g) when compared with the prismatic tube of same thickness which had a SEA of 17.06(J/g). At the same time the PCF transmitted to the structure is less among all the optimized tubes i.e. 16061.2 N. Hence this tube performs best among all the other tubes.

- The optimized tubes with a thickness of 1.5 and 2mm are shown to absorb almost the same amount of energy with decreasing SEA and increasing PCF. Thus the performance of these tubes is not desirable.
- Comparing the prismatic tube of 1mm thickness which was considered for performing topology optimization with the optimized tube of 1mm thickness the increment in SEA observed is 59.55% and reduction in the PCF and MCF transmitted was 48.48% and 43.17%.

REFERENCES

1. Huang, Xinyan, Y. M. Xie, and G. Lu. "Topology optimization of energy-absorbing structures." International Journal of crashworthiness 12, no. 6 (2007): 663-675.
2. Chen, B. C., M. Zou, G. M. Liu, J. F. Song, and H. X. Wang. "Experimental study on energy absorption of bionic tubes inspired by bamboo structures under axial crushing." International Journal of Impact Engineering 115 (2018): 48-57.
3. Sun, Guangyong, Hao Jiang, Jianguang Fang, Guangyao Li, and Qing Li. Crashworthiness of vertex based hierarchical honeycombs in out-of-plane impact." Materials & Design 110 (2016): 705-719.
4. Zhang, Yong, Minghao Lu, Chun H. Wang, Guangyong Sun, and Guangyao Li. "Out-of-plane crashworthiness of bio-inspired self-similar regular hierarchical honeycombs." Composite Structures 144 (2016): 1-13.
5. Tsang, H. H., and S. Raza. "Impact energy absorption of bio-inspired tubular sections with structural hierarchy." Composite Structures 195 (2018): 199-210.
6. Hu, Dayong, Yongzhen Wang, Bin Song, Linwei Dang, and Zhiqiang Zhang. "Energy-absorption characteristics of a bionic honeycomb tubular nested structure inspired by bamboo under axial crushing." Composites Part B: Engineering 162 (2019): 21-32.
7. Tarlochan, F., F. Samer, A. M. S. Hamouda, S. Ramesh, and Karam Khalid. "Design of thin wall structures for energy absorption applications: enhancement of crashworthiness due to axial and oblique impact forces." Thin-Walled Structures 71 (2013): 7-17.
8. Asanjarani, A., A. Mahdian, and S. H. Dibajian. "Comparative analysis of energy absorption behavior of tapered and grooved thin-walled tubes with the various geometry of the cross section." Mechanics of Advanced Materials and Structures (2018): 1-12.
9. Yamashita, Minoru, Manabu Gotoh, and Yasuhiko Sawairi. "Axial crush of hollow cylindrical structures with various polygonal cross-sections: Numerical simulation and experiment." Journal of Materials Processing Technology 140, no. 1-3 (2003): 59-64.
10. Abolfathi, Mostafa, and Ali Alavi Nia. "Optimization of energy absorption properties of thin-walled tubes with combined deformation of folding and circumferential expansion under axial load." Thin-Walled Structures 130 (2018): 57-70.
11. Marzbanrad, Javad, and Mohammad Reza Ebrahimi. "Multi-objective optimization of aluminum hollow tubes for vehicle crash energy absorption using a genetic algorithm and neural networks." Thin-Walled Structures 49, no. 12 (2011): 1605-1615.
12. Ahmed, Naveed, Pu Xue, Muhammad Kamran, Naeem Zafar, Ammara Mustafa, and M. S. Zahran. "Investigation of the energy absorption characteristics of metallic tubes with curvy stiffeners under dynamic axial crushing." Latin American Journal of Solids and Structures 14, no. 8 (2017): 1443-1463.
13. Ding, Xueshan, Zeqi Tong, Yang Liu, and Shutian Liu. "Dynamic axial crush analysis and design optimization of a square multi-cell thin-walled tube with lateral variable thickness." International Journal of Mechanical Sciences 140 (2018): 13-26.
14. Bigdeli, Ali, and Mohammad Damghani Nouri. "A crushing analysis and multi-objective optimization of thin-walled five-cell structures." Thin-Walled Structures 137 (2019): 1-18.

15. Luo, Yonghao, and Hualin Fan. "Energy absorbing ability of rectangular self-similar multi-cell sandwich-walled tubular structures." Thin-Walled Structures 124 (2018): 88-97.
16. Xu, Xiang, Yong Zhang, Jin Wang, Feng Jiang, and Chun H. Wang. "Crashworthiness design of novel hierarchical hexagonal columns." Composite Structures 194 (2018): 36-48.
17. Deng, Xiaolin, and Wangyu Liu. "Multi-objective optimization of thin-walled sandwich tubes with lateral corrugated tubes in the middle for energy absorption." Thin-Walled Structures 137 (2019): 303-317.
18. Salehghaffari, S., M. Tajdari, M. Panahi, and F. Mokhtarnezhad. "Attempts to improve energy absorption characteristics of circular metal tubes subjected to axial loading." Thin-Walled Structures 48, no. 6 (2010): 379-390.
19. Ming, Shizhao, Caihua Zhou, Tong Li, Zhibo Song, and Bo Wang. "Energy absorption of thin-walled square tubes designed by kirigami approach." International Journal of Mechanical Sciences 157 (2019): 150-164.
20. Nia, A. Alavi, and M. Parsapour. "Comparative analysis of energy absorption capacity of simple and multi-cell thin-walled tubes with triangular, square, hexagonal and octagonal sections." Thin-Walled Structures 74 (2014): 155-165.
21. Li, Zhigang, Haifeng Yang, Xiongwei Hu, Jifei Wei, and Zhitong Han. "Experimental study on the crush behavior and energy-absorption ability of circular magnesium thin-walled tubes and the comparison with aluminum tubes." Engineering Structures 164 (2018): 1-13.
22. Marzbanrad, Javad, Mehdi Mehdikhanlo, and Ashkan Saeedi Pour. "An energy absorption comparison of square, circular, and elliptic steel and aluminum tubes under impact loading." Turkish Journal of Engineering and Environmental Sciences33, no. 3 (2010): 159-166.
23. Wang, Yifan, Jiusheng Feng, Jianghao Wu, and Dayong Hu. "Effects of fiber orientation and wall thickness on energy absorption characteristics of carbon-reinforced composite tubes under different loading conditions." Composite Structures 153 (2016): 356-368.
24. Al Galib, D., and A. Limam. "Experimental and numerical investigation of static and dynamic axial crushing of circular aluminum tubes." Thin-Walled Structures 42, no. 8 (2004): 1103-1137.
25. Patankar, S. N., and Tan Ming Jen. "Strain rate insensitive plasticity in aluminum alloy 5083." Scripta Materialia 38, no. 8 (1998).
26. Zarei, H. R., and M. Kröger. "Multiobjective crashworthiness optimization of circular aluminum tubes." Thin-walled structures 44, no. 3 (2006): 301-308.

